

Effect of Relative Humidity on the Crystallization of Sol–Gel Lanthanum Zirconium Oxide Films

S. Sathyamurthy,^{*,†,‡} K. Kim,[†] T. Aytug,^{†,§} and M. Paranthaman[†]

Oak Ridge National Laboratory, Oak Ridge, Tennessee 37831, and Center for Materials Processing, Department of Materials Science and Engineering, and Department of Physics, University of Tennessee, Knoxville, Tennessee 37996

Received August 17, 2006

Revised Manuscript Received October 26, 2006

Sol–gel processing is a versatile solution based processing approach for the synthesis of a variety of ceramic oxides. The main attraction of this process is the flexibility and control it offers in terms of stoichiometry, microstructure, and crystallographic texture. This process has been used to synthesize a variety of technologically important oxides such as PbTiO_3 ,^{1,2} BaTiO_3 ,³ $\text{Pb}(\text{Zr,Ti})\text{O}_3$ (PZT),⁴ $\text{SrBi}_2\text{Ta}_2\text{O}_9$ (SBT),⁵ and so forth. In our work, we have extended this approach to deposit highly oriented films of RE_2O_3 ,⁶ RE-zirconates,⁷ RE-niobates,⁸ and so forth, on biaxially textured Ni–alloy substrates. In the area of coated conductor fabrication, there is a need for highly oriented films that can act as a buffer layer to prevent interdiffusion between the metal substrate and the $\text{YBa}_2\text{Cu}_3\text{O}_{7-d}$ (YBCO) superconductor film.⁹ A non-vacuum, scaleable process such as sol–gel processing could be ideally suited for the deposition of these buffer layers over long lengths of tapes because of the significant cost advantages it offers. In our previous work we have shown that lanthanum zirconium oxide (LZO) is an effective buffer layer for processing coated conductors with critical currents greater than 250 A/cm, which is the state-of-the-art for LZO processing.⁷ Other researchers are also exploring the use of LZO as a buffer layer in coated conductors.¹⁰ During the processing of 0.8 μm thick YBCO

films by metal organic deposition (MOD), the diffusion of Ni was found to be contained within the first 75 nm of the LZO film.⁷ However, to be viable as a stable manufacturing process, a complete understanding of the various process variables that need to be regulated is imperative. In this paper, we investigate the effect of relative humidity during the coating step on the texture and microstructure of sol–gel processed LZO thin films.¹¹

X-ray diffraction (XRD) patterns obtained for samples spin coated under relative humidity ranging from 10% to 80%, and processed at 1100 °C for 15 min are illustrated in Figure 1. The intensity of the LZO (222) peak, which gives an estimate of the amount of random polycrystalline fraction in the film, decreases as the relative humidity during the coating process is increased, dropping to background levels when relative humidity of 40% or above is used. Similar trends were also seen at 900 and 1000 °C process temperatures. Figure 2 illustrates the percentage of random polycrystalline material in the films as a function of relative humidity at various temperatures. The effect of humidity on the percentage of random polycrystalline material seems to be less exaggerated at lower temperatures. However, since all samples were processed only for 15 min, the lower amount of random material at lower temperatures could be due to slower crystallization kinetics. As the amount of random-oriented material decreases a concomitant increase in the amount of cube-textured material [lower bounds calculated using the pole figures from the LZO (222) peak] is observed. This is illustrated for samples processed at 1100 °C for 15 min in Figure 3.

Figure 4 shows the reflection high energy electron diffraction (RHEED) patterns collected from samples processed at 900 °C and 1100 °C after coating at 20% and 40% humidity levels. Samples coated at 40% relative humidity show a clean spot pattern showing a fully oriented material

[†] Oak Ridge National Laboratory.

[‡] Center for Materials Processing, Department of Materials Science and Engineering, University of Tennessee.

[§] Department of Physics, University of Tennessee.

- (1) Bao, Y.; Yao, X.; Shinozaki, K.; Mizutani, N. *J. Phys. D: Appl. Phys.* **2003**, *36*, 2141.
- (2) Sirera, R.; Calzada, M. L. *Mater. Res. Bull.* **1995**, *30*, 11.
- (3) Hayashi, T.; Ohji, N.; Hirohara, K.; Fukunaga, T.; Maiwa, H. *Jpn. J. Appl. Phys.* **1993**, *32*, 4092.
- (4) Dey, S. K.; Budd, K. D.; Payne, D. A. *IEEE Transactions on Ultrasonics, Ferroelectrics, and Frequency Control* **1988**, *35*, 80.
- (5) Koiwa, I.; Kanehara, T.; Mita, J.; Iwabuchi, T.; Osaka, T.; Ono, S.; Maeda, M. *Jpn. J. Appl. Phys.* **1996**, *35*, 4946.
- (6) Morrell, J. S.; Xue, Z. B.; Specht, E. D.; Goyal, A.; Martin, P. M.; Lee, D. F.; Feenstra, R.; Verebelyi, D. T.; Christen, D. K.; Chirayil, T. G.; Paranthaman, M.; Vallet, C. E.; Beach, D. B. *J. Mater. Res.* **2000**, *15*, 621.
- (7) Sathyamurthy, S.; Paranthaman, M.; Heatherly, L.; Martin, P. M.; Goyal, A.; Kodenkandath, T.; Li, X.; Rupich, M. W. *J. Mater. Res.* **2006**, *21*, 910.
- (8) Bhuiyan, M. S.; Paranthaman, M.; Sathyamurthy, S.; Goyal, A.; Salama, K. *J. Mater. Res.* **2005**, *20*, 904.
- (9) Rupich, M. W.; Verebelyi, D. T.; Zhang, W.; Kodenkandath, T.; Li, X. P. *MRS Bull.* **2004**, *29*, 572.
- (10) Knoth, K.; Huhne, R.; Oswald, S.; Schultz, L.; Holzapfel, B. *Supercond. Sci. Technol.* **2005**, *18*, 334.

- (11) Experimental details: The sol–gel precursor solution was prepared from alkoxides of lanthanum and zirconium. Lanthanum isopropoxide (Alfa, La 40% assay), zirconium *n*-propoxide in *n*-propanol (Alfa, 70%, w/w), and 2-methoxyethanol (Alfa, spectrophotometric grade) were used as received. For 20 mL of 0.75 M solution, stoichiometric quantities of lanthanum isopropoxide (2.37 g) and zirconium *n*-propoxide (3.51 g) were dissolved in 2-methoxyethanol and refluxed in 40 mL of excess 2-methoxyethanol using a Schlenk-type apparatus. After multiple solvent exchanges, the final volume of the solution was reduced to 20 mL. LZO films were prepared by spin coating the precursor solution onto Ni–5 atom % W substrates (1 cm \times 1 cm) with a 75 nm Y_2O_3 seed layer using a spin speed of 2000 rpm for 30 s. The spin coating was carried out in a controlled humidity environment (using ETS model 5100 humidifier) with relative humidity changing from 10% to 80% at 23 °C. The samples were crystallized by introducing them directly into a preheated furnace after purging with Ar–4% H_2 for 3 min. This approach yields a ramp rate greater than 300 °C/min. The samples were heat treated immediately after coating without any pyrolysis step to burn off the organics. The coated films were crystallized at temperatures from 900 to 1100 °C for 15 min in a flowing atmosphere of Ar–4% H_2 gas. These conditions yield a LZO film thickness of 75 nm. The phase purity and texture of the samples were analyzed using XRD with a Philips XRG3100 diffractometer and a Picker four-circle diffractometer, respectively, using $\text{Cu K}\alpha$ radiation. The microstructure of the samples was characterized using a field emission scanning electron microscope. The surface crystallinity and roughness of the samples were characterized using RHEED and AFM in contact mode, respectively.

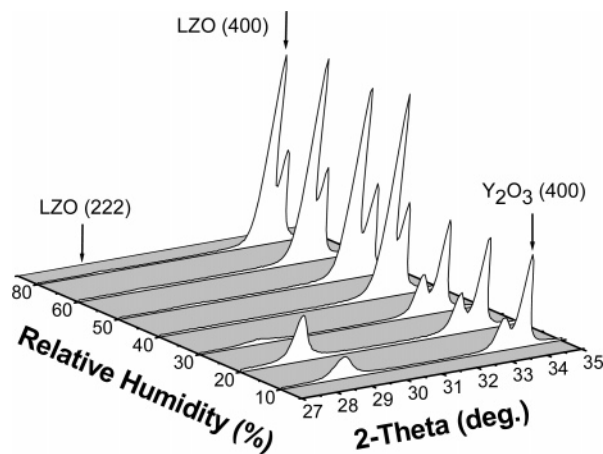


Figure 1. XRD patterns of samples coated under different relative humidity levels (10–80%) and processed at 1100 °C for 15 min.

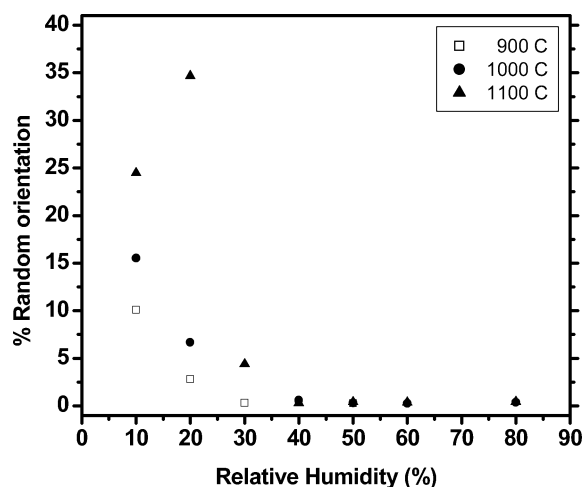


Figure 2. Variation of percent random polycrystalline material as a function of relative humidity during coating for a series of processing temperatures.

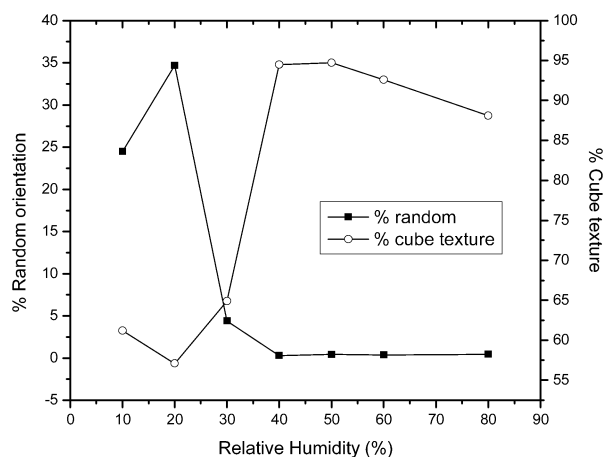


Figure 3. Variation of percent randomly oriented and cube textured material in the films as a function of relative humidity for samples processed at 1100 °C for 15 min.

at both temperatures. The pattern obtained from the sample coated at 20% relative humidity and processed at 1100 °C shows a mixture of spots and rings suggesting a mixture of oriented and random material at the surface of the sample. In contrast, the sample coated at 20% relative humidity and processed at 900 °C for 15 min shows no diffraction pattern, suggesting that the surface of the film is completely amorphous. This observation is consistent with the observa-

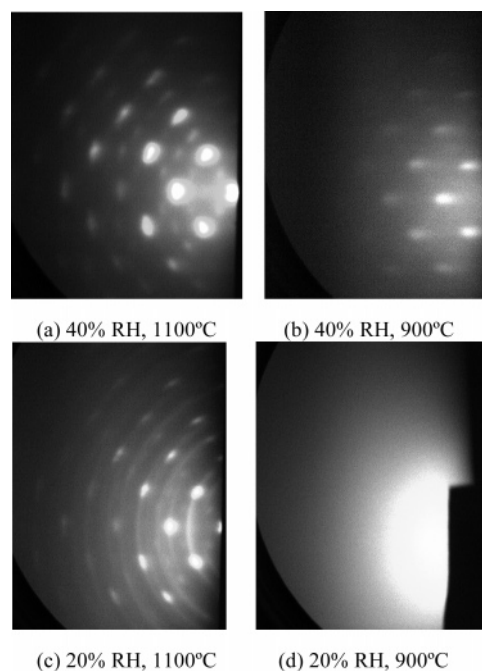


Figure 4. RHEED patterns for LZO samples processed at different values of relative humidity and temperature.

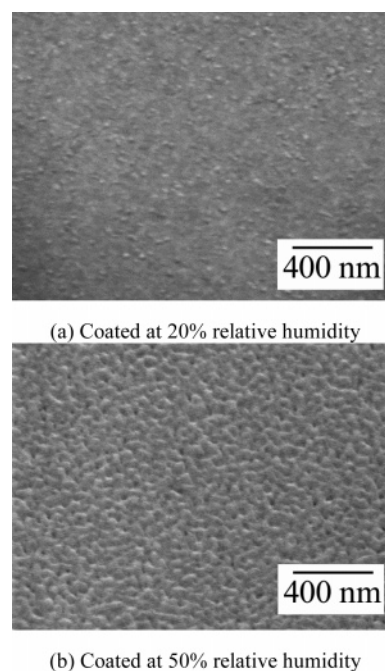


Figure 5. Effect of relative humidity during coating on the microstructure for samples processed at 1100 °C for 15 min illustrated using scanning electron microscopy images.

tions using XRD suggesting that, at lower humidity levels, the LZO film is not completely crystallized at 900 °C. Apart from the differences in electron and X-ray diffraction patterns of samples coated under different relative humidity levels, a clear difference was also observed in the microstructure of the films. Figure 5 shows the SEM microstructures of two LZO films processed at 1100 °C for 15 min coated at two different humidity levels (Figure 5a, 20%, and Figure 5b, 50%). In samples coated with optimal humidity levels a pronounced granularity was seen at the surface, while samples processed at lower humidity showed mostly smooth surface with a few particulates distributed randomly on the

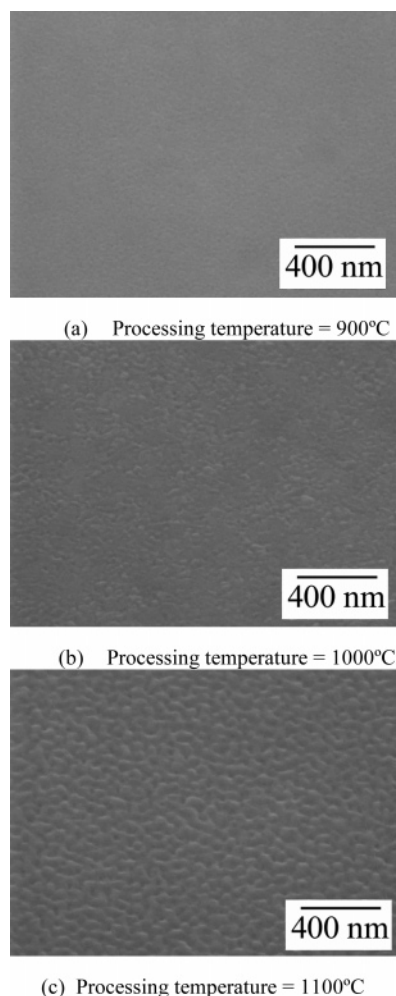


Figure 6. Effect of processing temperature on the microstructure of the samples coated at 40% relative humidity illustrated using scanning electron microscopy images.

surface. The amount of particulates observed was found to decrease with the processing temperature. For samples coated under optimal humidity, the granularity in the microstructure was found to be less severe with decrease in processing temperature (Figure 6). This is consistent with atomic force microscopy (AFM) roughness measurements, where the surface roughness decreased from 1.95 to 1.21 nm to 0.37 nm for samples processed at 1100 °C, 1000 °C, and 900 °C, respectively.

The effect of hydrolysis water on the orientation and microstructure of sol-gel films has been studied on several oxides such as PbTiO_3 ,^{12,13} PZT ,¹³ $\text{Ba}_x\text{Sr}_{1-x}\text{TiO}_3$,¹⁴ LiNbO_3 ,¹⁵ and so forth. In all these studies, typically, hydrolysis has

been reported to cause a decrease in epitaxy by promotion of homogeneous nucleation which competes with the heterogeneous nucleation at the substrate surface (film-substrate interface). The effect seen here is quite different from the hydrolysis effects reported by others. This suggests that the effect of relative humidity should not be due to hydrolysis. The present results seem to indicate that, for this system, there is a threshold humidity level that is required for complete epitaxial nucleation and growth. In samples coated at low humidity, as a result of an insufficient amount of moisture at the interface, the extent of epitaxial nucleation may be reduced. Thus, other modes of nucleation (with random orientation) at the film surface, substrate surface, and film bulk may become active. On the other hand, above a threshold humidity level there would be a uniform distribution of moisture throughout the thickness, and since epitaxial nucleation and growth initiated from the substrate surface are energetically favored, the dominant mode of crystallization should be through epitaxial nucleation at the substrate surface. Further studies on the changes to the chemical nature of the amorphous precursor film as a function of coating humidity may help elucidate the reasons for the effects reported in this work. Once this study is complete, an additional manuscript providing a detailed discussion on this topic will be published.

Acknowledgment. The authors would like to thank American Superconductor Corporation, Westborough, MA, for providing Y_2O_3 coated Ni-5 atom % W textured substrates. This work was sponsored by the Department of Energy, Office of Basic Energy Sciences, Division of Materials Sciences, Office of Electricity Delivery and Energy Reliability (OE). This research was performed at the Oak Ridge National Laboratory, managed by UT-Battelle, LLC, for the U.S. Department of Energy under Contract No. DE-AC05-00OR22725U.S.

Supporting Information Available: In-plane and out-of-plane texture data for the samples processed at various temperatures and relative humidity, calculation of percent random orientation, calculation of percent cube texture, and AFM scans (PDF). This material is available free of charge via the Internet at <http://pubs.acs.org>.

CM0619353

- (12) Schwartz, R. W. *Chem. Mater.* **1997**, 9, 2325.
- (13) Chen, S. Y.; Chen, I. W. *J. Am. Ceram. Soc.* **1994**, 77, 2332.
- (14) Hasenkox, U.; Hoffman, S.; Waser, R. *J. Sol.-Gel Sci. Technol.* **1998**, 12, 67.
- (15) Nashimoto, K.; Cima, M. J.; McIntyre, P. C.; Rhine, W. E. *J. Mater. Res.* **1995**, 10, 2564.